

See discussions, stats, and author profiles for this publication at: <https://www.researchgate.net/publication/24434677>

# Aging and Metastability of Monoglycerides in Hydrophobic Solutions

ARTICLE *in* LANGMUIR · JUNE 2009

Impact Factor: 4.46 · DOI: 10.1021/la9002065 · Source: PubMed

---

CITATIONS

30

READS

37

## 2 AUTHORS:



Chia-Hung Chen  
National University of Singapore  
32 PUBLICATIONS 589 CITATIONS

[SEE PROFILE](#)



Eugene M Terentjev  
University of Cambridge  
304 PUBLICATIONS 7,463 CITATIONS

[SEE PROFILE](#)

## Aging and Metastability of Monoglycerides in Hydrophobic Solutions

C. H. Chen and E. M. Terentjev\*

Cavendish Laboratory, University of Cambridge, JJ Thomson Avenue, Cambridge CB3 0HE, United Kingdom

Received January 17, 2009. Revised Manuscript Received April 23, 2009

Monoglyceride dispersed in oil acts as gel emulsifier to stabilize ordered lamellar structures; however, with time these phases age, leading to separation of oil and lipid. The aging of aggregated structures of monoglycerides in hydrophobic medium is described by a set of different techniques. Polarized microscopy was used to study the mesomorphic behavior as a function of time. Differential scanning calorimetry was utilized to quantitatively monitor changes in the latent heat in different phase transformations that take place in the aging system. The X-ray diffraction patterns fingerprinted the molecular arrangement in different emerging phases. Infrared spectroscopy was used to monitor the states of hydrogen bonding in the system. We conclude that in both inverted-lamellar and sub- $\alpha$  crystalline phases, monoglyceride molecules inevitably lose their emulsified ability in the hydrophobic solutions through the gradual change in hydrogen bonding patterns. On aging, the recombination of hydrogen bonding between glycerol groups causes the segregation of chiral (D and L) isomers within the bilayers. Therefore, all structures were eventually forced to reorder into the ground-state  $\beta$ -crystalline phase. Accordingly, the highly ordered packing of aged structures weakened the emulsifying ability and finally led to the collapse of the percolating gel network.

### 1. Introduction

Monoglycerides (MG) are lipid molecules consisting of a single fatty acid esterified with a 1-hydroxy glycerol group (see Figure 1). They are distinguished by the length of carbon chain. In this paper, we focus on a particularly common surfactant, monostearate C18. Unlike typical nonionic surfactants, MG is an optically active molecule that exists in two chiral isomers: D and L.<sup>1,2</sup> Concentrated mixtures of MG in solvents form cream-like materials widely used both in personal products and in food industries.<sup>3,4</sup> Attractive features of MG dispersed in oil include two main factors: uniquely, these molecules form an elastic gel network on initial aggregation on cooling from the isotropic liquid into the lamellar phase, which then retains its mechanical stability on further cooling.<sup>5</sup> In practical applications, partly due to this mechanical stability and partly due to their biocompatibility, MG/oil mixtures could be used in healthy food products as substitutes for butter. Due to the absence of water, MG/oil systems are not very susceptible to microbial infection and auto-oxidation and thus can be stored at room temperature without the need for preservative additives.<sup>6–9</sup> Beyond their use in various applications, in general, aggregated surfactant

solutions form a particular class of materials that develop a network of morphological features to retain the solvent.<sup>10,11</sup> For these reasons, the detailed knowledge of MG/oil morphology and dynamics is important for both scientific advancement and technological implementation.

MG systems have been studied systematically for many years. The structure of pure MG was first described by Larsson in 1966<sup>12</sup> and was later reviewed by Small (1986),<sup>13</sup> Larsson (1994),<sup>14</sup> and Krog (2001).<sup>15</sup> The rich polymorphic behavior of MG/water is well-established. Upon temperature decrease, the emerging phases could be divided into three groups.<sup>2,16</sup> In the high-temperature region, the material is in the isotropic fluid phase (which may involve miscellaneous micellar aggregation). At a lower temperature, the lamellar phase exists over a wide range of concentrations.<sup>1</sup> According to the literature, below the Krafft temperature,  $T_K$ , the lamellar phase transforms into the  $\alpha$ -crystalline phase characterized by the hexagonal surfactant packing in layers with a single spacing at 4.18 Å.<sup>17,18</sup> Results of our recent work<sup>5</sup> indicate that the same structural feature is seen in the inverse-lamellar phase of MG in the oil matrix, where the characteristic 4.17 Å spacing arises from the hexagonal ordering of glycerol heads in the tightly compressed midbilayer planes (while the aliphatic tails remained amorphous, although laterally densely packed). Since the characteristically concentration-independent Krafft point  $T_K$  involves crystallization on demixing, we are concerned about the structural interpretation of the  $\alpha$ -phase in aqueous systems; however, this is not the subject of the present article, which deals with purely nonaqueous systems. A detailed

\*emt1000@cam.ac.uk.

(1) Cassin, G.; de Costa, C.; van Duynhoven, J. P. M.; Agterof, W. G. M. *Langmuir* **1998**, *14*, 5757–5763.

(2) Gehlert, U.; Vollhardt, D.; Brezesinski, G.; Mohwald, H. *Langmuir* **1996**, *12*, 4892–4896.

(3) van Duynhoven, J. P. M.; Broekmann, I.; Sein, A.; van Kempen, G. M. P.; Goudappel, G. J. W.; Veenman, W. S. J. *Colloid Interface Sci.* **2005**, *285*, 703–710.

(4) Heertje, I.; Roijers, E. C.; Hendrickx, H. A. C. M. *Lebensm-Wiss Technol.* **1998**, *31*, 387–396.

(5) Chen, C. H.; Terentjev, E. M. *Soft Matter* **2009**, *5*, 432–439.

(6) Ojijo, N. K.; Neeman, I.; Eger, S.; Shimoni, E. *J. Sci. Food Agric.* **2004**, *84*, 1585–1593.

(7) Ojijo, N. K.; Kesselman, E.; Shuster, V.; Eichler, S.; Eger, S.; Neeman, I.; Shimoni, E. *Food Res. Int.* **2004**, *37*, 385–393.

(8) Kesselman, E.; Shimoni, E. *Food Biophys.* **2007**, *2*, 117–123.

(9) Sagalowicz, L.; Leser, M. E.; Watzke, H. J.; Michel, M. *Trends Food Sci. Technol.* **2006**, *17*, 204–214.

(10) Sein, A.; Verheij, J. A.; Agterof, W. G. M. *J. Colloid Interface Sci.* **2002**, *249*, 412–422.

(11) Murdan, S.; Gregoriadis, G.; Florence, A. T. *J. Pharm. Sci.* **1999**, *88*, 608–614.

(12) Larsson, K. *Acta Crystallogr.* **1966**, *21*, 267–272.

(13) Small, D. M. *The Physical Chemistry of Lipids*; Marcel Dekker: New York, 1986; pp 386–392, 475–492.

(14) Larsson, K. *Molecular Organisation, Physical Functions and Technical Applications*; Oily Press: Bridgwater, 1994.

(15) Krog, N. *Crystallization Processes in Fats and Lipid Systems*; Marcel Dekker: New York, 2001; Chapter 15, pp 505–519.

(16) Kros, N.; Larsson, K. *Chem. Phys. Lipids* **1968**, *2*, 129–143.

(17) Marangoni, A. G.; Narine, S. S. *Physical Properties of Lipids*; Marcel Dekker: New York, 2001; pp 292–307, 324–336.

(18) Batte, H. D.; Wright, A. J.; Rush, J. W.; Idziak, S. H. J.; Marangoni, A. G. *Food Biophys.* **2007**, *2*, 29–37.

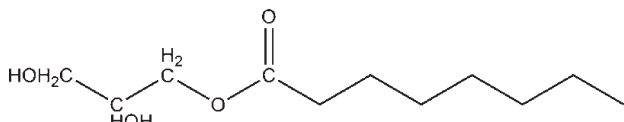


**Figure 1.** 1-Monoglyceride is a lipid molecule consisting of a fatty acid esterified with a 1-hydroxy glycerol group, which contains two hydroxide groups (OH). One OH is at the end of the head (3-OH); the other is attached at the second carbon (2-OH). These two groups give the complex hydrogen bonding interaction in MG systems.

study of the headgroup hydration revealed that there were three water molecules bonded to one surfactant molecule in the lamellar phase.<sup>19</sup> In the  $\alpha$ -crystalline state, these three bonds reduced to one and, as a result, weakened the emulsification ability. Moreover, the stability of the MG gel network was mainly governed by the van der Waals attraction force and short-range repulsive between bilayers.<sup>20,21</sup> The repulsive pressure between bilayers in the  $\alpha$ -crystalline phase was significantly smaller than the pressure in the lamellar phase, leading to compaction of bilayers.

The initial  $\alpha$ -crystalline gel is metastable and readily transforms into an anhydrous MG crystal, identified as the  $\beta$ -crystalline state (often called the “coagel”),<sup>1,3</sup> which has a higher melting point and is characterized by several wide-angle X-ray reflections reflecting short spacings in the unit cell, with the strongest line corresponding to 4.5–4.6 Å.<sup>15,13</sup> A coagel state of MG in water is believed to be due to hydrogen bonds being established between glycerol head groups in bilayers, which in turn leads to a further crystallization of aliphatic tails.<sup>1</sup> On a long time scale of aging, the D- and L-isomers of chiral MG gradually separate within crystalline bilayers, leading to more dense packing and expulsion of water. Sedimentation of solid in this phase then takes place.

Compared with the aqueous systems, MG in a purely hydrophobic solvent is much less studied. The rheology and storage properties have been reported in a series of papers by Shimoni et al.<sup>6–8</sup> However, due to the absence of confident structure descriptions, the mechanism of aging phenomena remained unclear. There are many examples of the use of ternary MG/water/oil systems.<sup>18,22–27</sup> However, the presence of water would dominate the phase behavior of aggregating MG even at the lowest water content (0.5% w/w). In our recent work, we have studied MG C18 in oil in the absence of water.<sup>5</sup> Having checked the effect of very small amounts of water added to a completely desiccated MG/oil mixture, we have been able to establish the boundary of the water content, below which the hydrophobic mixture may be regarded as “dry”, and above which the effect of water becomes increasingly significant. This boundary lies at about 0.2% w/w and could be easily understood by verifying the mole concentrations: the change in phase behavior occurs when there is, crudely, one water molecule for each molecule of MG.<sup>5</sup>

- (19) Morley, W. G.; Tiddy, G. J. T. *Chem. Soc. Faraday Trans.* **1993**, *89*, 2823–2831.
- (20) Pezron, I.; Pezron, E.; Bergenstahl, B. A.; Claesson, P. M. *J. Phys. Chem.* **1990**, *94*, 8255–8261.
- (21) McIntosh, T. J.; Magid, A. D.; Simon, S. A. *Biophys. J.* **1989**, *55*, 897–904.
- (22) Guillot, S.; Moitzi, C.; Salentning, S.; Sagalowicz, L.; Leser, M. E.; Glatter, O. *Colloids Surf., A* **2006**, *291*, 78–84.
- (23) Marangoni, A. G.; Idziak, S. H. J.; Vega, C.; Batte, H.; Ollivon, M.; Jantzi, P. S.; Rush, W. E. *Soft Matter* **2007**, *3*, 183–187.
- (24) Batte, H. D.; Wright, A. J.; Rush, J. W.; Idziak, S. H. J.; Marangoni, A. G. *Food Res. Int.* **2007**, *40*, 982–988.
- (25) Patin, J. M. R.; Nino, M. R. R.; Sanchez, C. C.; Garcia, J. M. N.; Mateo, G. R. R.; Fernandez, M. C. *Colloids Surf., B* **2001**, *21*, 87–99.
- (26) Sari, P.; Razzak, M.; Tucker, I. G. *Int. J. Pharm.* **2003**, *270*, 287–296.
- (27) Krog, N.; Larsson, K. *Fett. Wiss. Technol.* **1990**, *2*, 54–57.

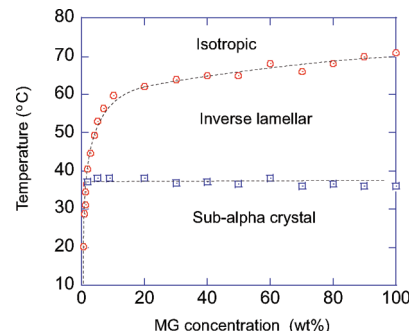


**Figure 2.** The phase diagram of MG C18 in oil showed three phases between 0 and 80 °C: isotropic, inverse lamellar, and sub- $\alpha$  crystalline phases. The crystallization temperature,  $T_K$ , is characteristically independent of concentration.

Working consistently in dry conditions, in the sense specified above, we have established a reasonably universal phase diagram (Figure 2). Due to the difference in hydrogen bonding patterns, MG/oil showed phase behavior very different from the aqueous systems. Below the isotropic-lamellar transition temperature,  $T_L$ , the inverse lamellar phase was formed, as expected in the hydrophobic system. However, due to the unique size ratio between the glycerol head and the lateral area of the aliphatic chain in the fully extended dense brush, the inverse lamellar bilayers have a very definite hexagonal in-plane ordering. We have concluded that this is a two-dimensional dense packing of glycerol heads, compressed in the middle of each bilayer. One might suggest that the hexagonal order arises from laterally densely packed aliphatic tails, e.g., ref 18. However, if we make a comparison with other densely grafted polymer brushes, and more importantly, other single-aliphatic tail surfactants, none of which have such a hexagonal packing, the much more likely scenario is that the glycerol heads are densely packed in 2D planes; and then, the tails (in the fully extended due to the high brush density, but nevertheless molten amorphous state) simply follow that effective grafting pattern. The wide-angle X-ray reflection at 4.17 Å corresponds to the closest distance of approach of glycerol groups in a plane. We have concluded that the second, “twin” peak at 4.11 Å is the characteristic distance between the neighboring heads in two planes of the bilayer. Continuously cooling down below the crystallization point of the surfactant, the lower-temperature phase transition emerges. Characteristically, this crystallization temperature does not depend on MG concentration, which suggests that this is the hydrophobic Krafft demixing point,  $T_K$ . The lateral hexagonal packing transformed into a structure analogous to the “sub- $\alpha$ ” crystalline phase known in aqueous systems, with orthorhombic chain packing in the unit cell, characterized by strong X-ray reflection at 4.17 Å and several reflections between 4.06 to 3.6 Å.<sup>5</sup> The reason the ordinary (in aqueous systems)  $\alpha$ -crystal state is not observed in the hydrophobic environment is that the highly 2D-ordered glycerol heads promote a higher degree of order on the subsequent crystallization of aliphatic tails, thus bypassing the  $\alpha$ -crystalline state, which still has hydrated glycerol groups on the outside of each bilayer.

This unique structural feature of the inverse lamellar phase is the origin of the well-known rheological feature of MG/oil systems: they form an elastic gel at a high temperature, immediately below the isotropic-lamellar transition. The structured bilayers have much less flexibility and thus form a percolating scaffold that can resist the macroscopic stress applied to the system. On entering the lower-temperature crystalline phase,

the elastic modulus of the gel was shown to not change significantly, although the yield stress of course does change due to the different bending rigidity of bilayers.

However, with the passing of time, the microscopic structure that MG molecules form in different phases changes, and this aging leads to a dramatic change of physical properties. Most importantly, the emulsifying ability of aggregated MG reduces and the oil separates from the more densely aggregated MG crystalline regions. In practice, this means that the phase diagrams, such as that presented in Figure 2, have only a representative meaning. This diagram, as all similar phase diagrams of MG/water or ternary systems that one finds in the literature, are obtained on cooling from the high-temperature isotropic solution when the corresponding phases first form, or on subsequently heating the system soon after (see the discussion of phase hysteresis in ref 5). Nevertheless, such an “apparent phase diagram” is a meaningful representation, because the aging times are rather long, as we shall see below. However, when approaching such phase diagrams one must be clear that the transition lines, and the nature of phases, do change with aging.

In the present work, we investigate the aging processes of MG/oil in both inverse-lamellar and sub- $\alpha$  crystalline phases. The textures and their evolution were observed through polarized microscopy. During aging, we find that the network structure breaks down into the isolated  $\beta$ -crystalline clusters dispersed in a continuous oil phase. Therefore, the lamellar network scaffold breaks down and phase separation between solid MG crystals and liquid oil takes place; as a result, the system loses its rheological characteristics of a gel. This aging process was quantitatively analyzed by a comparison of melting latent heat of transitions in aged and fresh materials, using differential scanning calorimetry (DSC). The structure of the  $\beta$ -crystal phase was characterized by X-ray diffraction. In order to understand the mechanism of aging, the time evolution of hydrogen bonding states was monitored by infrared spectroscopy. By comparing the relevant literature data and our infrared absorption peaks, we make conclusions about the rearrangement of hydrogen bonds during the aging process. Putting together results of several different experiments, we conclude that the MG/oil mixtures in both inverse-lamellar and sub- $\alpha$  crystalline phases are in fact metastable. Such a conclusion is expected for the sub- $\alpha$  crystalline phase (and corresponds to what takes places in aqueous systems); however, the metastability of the lamellar phase is an unusual finding. In both cases, with the passage of time the MG molecules rearrange into the true stable structure of the  $\beta$ -crystal, with alternating D and L MG layers. Accordingly, the highly ordered packing of aged structures weakened the emulsifying ability and caused the collapse of the gel network.

## 2. Experimental Details

Distilled saturated MG was purchased from the Palsgaard A/S (Denmark). In this work, we concentrate on the single sample mainly containing one characteristic saturated fatty acid, in contrast to other studies relevant to applications, where mixtures of lipids were used for better emulsification. The Palsgaard sample Dimodan 091 contains 97% monoglyceride (with 98% 1-MG and ~2% of 2-MG isomers) and the fatty acid chain length composition was 93% C18 (monostearin) and 7% C16 (monopalmitin). The remainder consisted of 1.1% diglycerides and less than 1% triglycerides. The hydrophobic solvent used in the bulk of this work was hazelnut oil from Provence, France, a variety which contains approximately 80% oleic and 20% linoleic acids with

low quantities of MG (see the detailed composition analysis in ref 28). This oil crystallizes at a temperature below -23 °C. Before testing, the hazelnut oil was heated to 120 °C for several hours to dry. The choice of this particular oil is partially dictated by practical applications. Later on, in the discussion of our results, one may question the extent to which the small impurity of the MG C18, and of the hazelnut oil, was important. From the earlier studies of equilibrium ordering,<sup>5</sup> we are clear that this is not important at all, and the conclusions are quite universal. As in that earlier study, here we have also carried out parallel tests on MG in *n*-tetradecane (the “model oil”) and found no significant changes in either infrared studies of hydrogen bonding or in calorimetric characterization of phase transitions (apart from a small shift of the lamellar transition temperature).

For this study, MG was mixed with the oil at a fixed concentration of 10% w/w. To ensure proper mixing, the solutions were placed on a magnetic stirrer heating plate at a constant temperature of 100 °C. In order to follow the aging in both sub- $\alpha$  crystalline and inverse lamellar phases, the samples were stored at 26 and 50 °C, respectively.

A Zeiss Axioplan microscope with crossed polarizers was attached to a Linkam TP91 hot stage unit. Samples of the 10% w/w MG/hazelnut oil were placed between a glass slide and a coverslip, with the thickness of the sample less than 0.5 mm. The sample was heated to 100 °C and annealed at this temperature for 5 min to eliminate thermal history. To observe the time evolution, samples were cooled from the isotropic phase and kept below relevant the transition temperature for two weeks.

Heat exchanges involved in a phase transition yielded exothermic or endothermic peaks that were recorded in a differential scanning calorimeter (DSC). From these measurements, the transition temperatures and the latent heat could be accurately estimated. A Perkin-Elmer power-compensated Pyris 1 differential scanning calorimeter equipped with an intracooler 2P was used. The samples for different periods of time were placed in the pans and heated to 100 °C from 26 °C (sub- $\alpha$  crystalline phase) or from 45 °C (inverse lamellar phase) to record the temperature and the latent heat on melting. After that, samples were held for 1 min at 100 °C and cooled to 0 °C, to assess the stability of the aged phase to melting nucleation. Each sample was measured in 40  $\mu$ L sealed aluminum pans at a scanning rate of 20 °C/min. The choice of this relatively high rate of temperature change was guided by the fact that we saw no qualitative differences in the transitions on testing at 10, 5, or 1 °C/min; but the sensitivity of DSC technique decreases dramatically, and our errors in determining the coagel index increased. All aging effects described here take a much longer time, while the initial lamellar ordering of the surfactant occurs sufficiently rapidly for us not to see a significant difference at varied cooling rates.

To determine the characteristics of hydrogen bonds, infrared absorption spectra were recorded employing a GALAX series 4020 FT-IR spectrometer (Thermal Electron Corporation, Waltham, MA, USA). The spectrometer was continuously purged excluding CO<sub>2</sub> from the sample holder box. The samples were placed in an IR cell between two NaCl windows. The temperature was regulated by placing the cell in a thermal stated holder controlled by a temperature controller (Eurotherm, SPECAC). To observe the thermal effects, the samples were prepared and the evolution of spectra was recorded from 20 to 100 °C with the interval of 10 °C, and then on cooling from 100 to 26 °C. After the heating treatment, the experiment was recorded continuously at room temperature every 24 h for 14 days to monitor the aging process.

X-ray scattering patterns were recorded using a copper rotating anode generator (Rigaku-MSC Ltd.) equipped with X-ray optics by Osmic Ltd. Before recording the X-ray diffraction, the samples were stored at 26 °C (crystalline phase) or at 50 °C

(28) Benitez-Sanchez, P. L.; Leon-Camacho, M.; Aparicio, R. *Eur. Food Res. Technol.* 2003, 270, 13–19.

(lamellar phase) for 14 days. The distance between the detector and the sample was set at 300 mm, giving a maximum resolution of 3.36 Å at the edge of the diffraction pattern. Samples were held between a mica sheet of 0.1 mm (supplied by Goodfellow, Cambridge, UK) and an aluminum plate. A metal substrate plate was used to ensure accurate heat transfer to the sample. The temperature was controlled by a homemade chamber and verified by a thermocouple.<sup>29</sup>

### 3. Aging Process

The aging of the textures in sub- $\alpha$  crystalline phase was observed by polarized optical microscopy. Figure 3 shows the typical microstructure at fixed temperature 26 °C, separated by a long period of aging. In order to record clear images, the sample thickness was less than 0.5 mm. As always, the samples were annealed at 100 °C and then cooled down to a certain temperature, after which the texture was recorded every 3 h for two days and subsequently every 12 h for two weeks. When the mixture was cooled to 26 °C, MG initially forms what we continue to call the “sub- $\alpha$  crystal” phase (by analogy with a similar structure in aqueous systems), which consists of dispersed crystalline bilayer plates making a polydomain percolating network throughout the sample. This texture shows bright birefringence under the crossed polarizers. The size of every elongated plate domain was roughly 100  $\mu\text{m}$  in length and 25  $\mu\text{m}$  in width. After a 10 day evolution (essentially slow recrystallization and phase separation from the residual oil), the structure changes into solid crystal clusters dispersed in a continuous oil phase. In this case, the gel-forming network is broken and the oil completely phase-separated from the MG crystals, which then gradually sediment by gravity.

The aging process could be followed thermodynamically by introducing a dimensionless number called the “coagel index” (CI), which is the ratio of the total latent heat of the transition in fresh and aged materials:  $\text{CI} = \Delta H(\text{aged})/\Delta H(\text{fresh})$ . The aged structure of aggregated MG contains  $\beta$ -crystals with a highly regular arrangement achieved through segregated molecular chirality. This causes the latent heat on melting the aged material to be higher than that in the freshly ordered system. Therefore, the CI could be used to monitor the fraction of the aged part in the sample by comparing the heat flow used to melt the freshly ordered and the aged material.

The result of our DSC study shows that CI increases gradually with the length of time the material spends at a low temperature, and eventually reaches saturation. In order to observe the time evolution of CI, the samples in these experiments were stored at a fixed temperature (26 °C) after quenching into the initial sub- $\alpha$  crystalline state. The typical DSC scans are presented in Figure 4a. As found in the earlier studies,<sup>5</sup> in the fresh sample one finds a sequence of two transition peaks on heating from 0 to 100 °C. The first peak corresponds to the melting of the crystallized carbon chains of sub- $\alpha$  crystals, and the second peak corresponds to the melting of the lamellar phase. After five days of aging at room temperature (26 °C), the two phase transitions displayed in the fresh sample essentially coalesced into one.

The melting enthalpy of aged  $\beta$ -crystalline samples was about 1.4 times the value obtained from melting the fresh samples (sub- $\alpha$  crystal). This 40% difference, and the evolution of CI on aging, is shown in Figure 4b. The initial value of  $\text{CI} = 1$  indicates the sample melting from the sub- $\alpha$  state, while the saturation value of 1.4 suggests the better-ordered  $\beta$ -crystalline state with a higher melting entropy. The time evolution of CI shows that the sub- $\alpha$

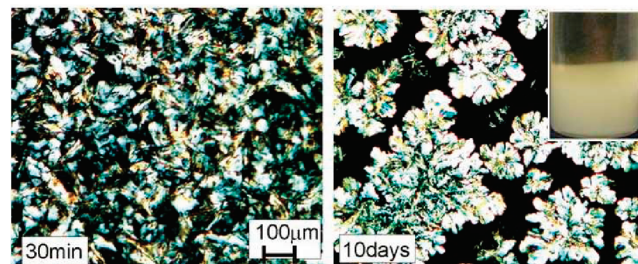


**Figure 3.** At 26 °C, MG initially aggregated into a lipid crystal network (elastic gel) that trapped the residual oil inside. After a 10 day evolution, the lamellar network was broken and crystalline regions aggregated together. The phases of oil and crystalline MG separate, which showed as a clear sedimentation boundary in the vessel (inset shows the 10 day old coagel).

phase is metastable and transformed into a more stable  $\beta$ -crystal arrangement over approximately 5–7 days.

In order to describe the molecular arrangement during aging at room temperature (26 °C), X-ray diffraction was employed to distinguish between the structures of fresh and aged samples, see Figure 5. The series of small angle reflections showed that both fresh and aged materials contained lamellar bilayers of approximately 49 Å thickness: the ratios of high-order small-angle reflections followed the characteristic sequence of 1, 1/2, 1/3, 1/4. Note that this spacing does not change on aging, as the crystalline bilayers keep their thickness (see ref 5 for detail of scattering intensity, including the broadband of scattering at wide angles which is the background due to the pure oil). The wide angle diffraction reveals the differences between phases. The fresh crystalline phase depicts sub- $\alpha$  ordering, which is characterized by the orthorhombic unit cell of chain packing with pronounced sequence of wide angle diffraction peaks at 4.27, 4.17, 4.09, 4.06, 3.95, and 3.62 Å.<sup>5,15</sup> The particularly strong reflection at 4.17 Å is the same as in the inverse-lamellar phase, which to us suggests that it originates from the 2D hexagonal packing of glycerol heads. After five days of aging, the material transforms to a  $\beta$ -crystal form. In this case, the all-trans zigzags of the alkyl chains are parallel with each other and the chains pack triclinically. The  $\beta$ -crystal form is characterized by two series of X-ray lines in the short-spacing region, 4.55, 4.51, 4.38, 4.26, 4.09, and 3.94, 3.84, 3.78, 3.60 Å.<sup>15</sup> One of these series (at wider angles) corresponds to the crystallized alkyl chains. We believe that the other series (at slightly smaller angles) reflects the correspondingly skewed periodic spacing between the glycerol heads in their planes.

Note that Figure 5 suggests that the glycerol head spacing was increased from 4.17 Å to 4.55 Å. This is an indication of the formation of intermolecular hydrogen bonding. During aging, 2-OH hydrogen bonds form between glycerol groups and force the molecules to rearrange their packing through separation of chiral isomers. Establishment of regular hydrogen bonds expands the local volume of each molecular head in the layer, and so increases the spacing between glycerol moieties, now mediated by the shared proton. This effect is analogous to what happens in the formation of ice from liquid water. Below the crystallization temperature, regular hydrogen bonds form between water molecules. These hydrogen bonds drive the rearrangement of water molecules into the lattice, and also expand the local volume (so the spacing between water molecules increases and the material density falls). The details of hydrogen bonding between MG molecules will be discussed in the following section.

(29) Goto, M.; Kozawa, K.; Uchida, T. *B. Chem. Soc. Jpn.* 1988, 61, 1434–1436.

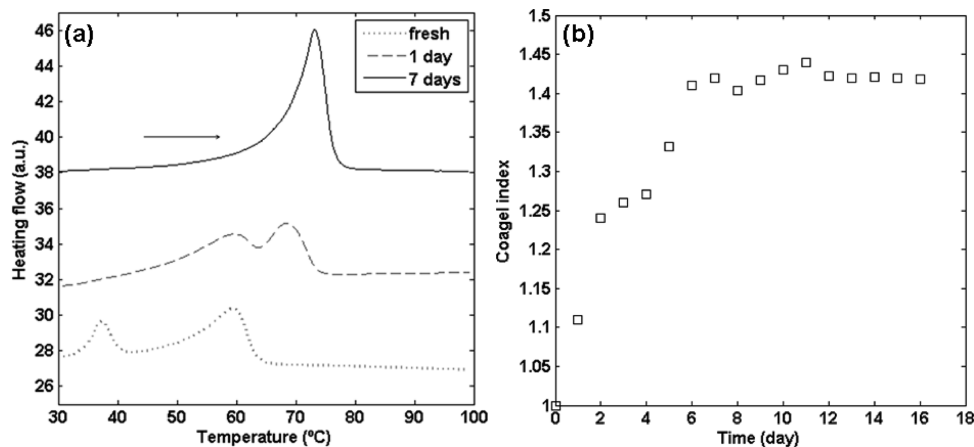


**Figure 4.** (a) First heating of the fresh sample shows two transition peaks corresponding to the melting of sub- $\alpha$  crystal and the lamellar phase. After one day at 26 °C, the DSC showed two peaks starting to coalesce. After five days, the sample changed to form  $\beta$ -crystals and exhibits only one melting peak at higher temperature, and changes no further. (b) CI increased gradually from 1.0 to 1.4 over approximately 5–7 days.

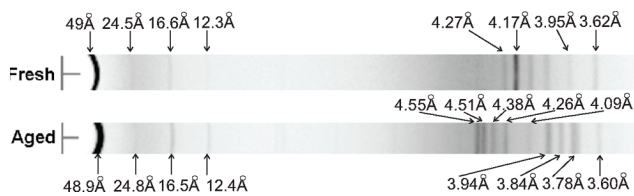


**Figure 5.** Sub- $\alpha$  crystalline phase is metastable and transforms into the stable  $\beta$ -crystal form during storage at ambient temperature. In the  $\beta$ -crystal, the alkyl chains are packed triclinically. The main spacing of glycerol head increases from 4.17 Å (sub- $\alpha$  crystal) to 4.55 Å ( $\beta$  crystal). This is evidence of the formation of 2-OH hydrogen bonds.

#### 4. Hydrogen Bonding

The state of hydrogen bonding was investigated by infrared spectroscopy. Spectra characterize absorption from specific molecular vibrations. In order to study hydrogen bonding of the hydroxide group, we focus on the low-energy region from 3000 to 4000 (1/cm) corresponding to the OH-stretching modes.<sup>30,31</sup> Due to the complex structure of hydrogen bonds in MG, there is very little literature available to determine the exact absorption peak positions of MG in oil. Due to the physical constraints, the vibration mode of 2-OH group shifts to a lower frequency with respect to the vibration band of the free alcohol-OH group.<sup>32</sup> Therefore, we have the twin absorption peaks corresponding to the 2-OH and 3-OH groups. Establishing hydrogen bonds for each of these groups shifts them further toward the low-energy range, which allows estimation of the strength of the hydrogen bond.<sup>31–33</sup>

Before the measurements, the samples were stored at 26 °C over one week to make sure their microstructure was completely aged to the  $\beta$ -crystalline state. Figure 6a shows a dominant absorption peak in 3250 (1/cm) and a secondary absorption peak around 3350 (1/cm) corresponding to 2- and 3-OH groups, respectively, bonded with the hydrogen bonds.<sup>35,31</sup> When the samples were

heated above 70 °C,  $\beta$ -crystals were melted directly into the isotropic fluid, giving two corresponding peaks at 3500 and 3550 (1/cm).<sup>33–35</sup> These twin peaks of OH-bond absorption are shifted to higher energy, which reflects the loss of hydrogen bonding. From this shift, we can estimate the strength of a hydrogen bond in MG, giving ~4.5 kcal/mol, which is slightly below the hydrogen bonding energy of pure glycerol.<sup>32</sup>

The corresponding cooling process was recorded after annealing the solution at high temperature and is shown in Figure 6b. On cooling, the material passed through three phases: isotropic fluid, inverse lamellar, and sub- $\alpha$  crystal. Below the gelation temperature (50 °C), MG aggregated into the inverse lamellar ordering. Hydrogen bonds were formed to alter the vibration frequency of the OH group, moving to lower frequency with increased intensity.<sup>31</sup> The freedom of 3-OH group relative to sterically hindered 2-OH group makes 3-OH form the hydrogen bond more easily with the neighboring C=O group. Therefore, the absorption peaks shifted from 3500, 3550, to 3350 (1/cm). By continuously cooling it down to 35 °C, the material was brought into the sub- $\alpha$  crystalline state. However, there was no visible change in hydrogen bonding: the infrared spectrum represented the same absorption as in the inverse lamellar phase.

To gain insight into the connection between aging and the formation of the hydrogen bonds between MG, the time evolution of the infrared spectrum was followed at room temperature (26 °C, see Figure 7). This shows the absorption band gradually splitting into two during aging. The new emerging peak is attributed to the hydrogen bond between alcohol (2-OH) and ester (C=O) groups, respectively. The 2-OH hydrogen bonding decreases the vibration frequency of molecules so the band shifts to a lower wavenumber at 3250 (1/cm). The coexistence of 3-OH and 2-OH hydrogen bonding is observed during aging; the lower-frequency band becomes sharper and increases its intensity (see Figure 7b). Over five days, the 2-OH bonding begins to dominate and eventually replaces the 3-OH bonds completely.

We thus conclude that 3-OH hydrogen bonding is not a stable link and only plays a subsidiary role in MG structuring. The 2-OH hydrogen bonds form and force rearrangement of MG in a more ordered way. D- and L-Isomers contain different orientations of hydroxide in the glycerol group. According to the literature, the 2-OH bonds between glycerol groups prefer to link the isomers that match the chiral orientation with each other to lower the overall free energy. Therefore, D- and L-isomers spontaneously select the same type of isomers, and this eventually promotes the

(30) Holmgren, A.; Lindblom, G.; Johansson, L. B. *A. J. Phys. Chem.* **1988**, 92, 5639–5644.

(31) Silverstein, R. M.; Bassler, G. C.; Morrill, T. C. *Spectrometric Identification of Organic Compounds*, 5th ed.; John Wiley: New York, 1991; pp 95–111, fig. 3.17.

(32) Atovmyan, E. G.; Koshchii, S. V.; Fedotova, T. N. *J. Appl. Chem.-USSR* **1988**, 48, 287–290.

(33) Susi, H.; Morris, S. G.; Scott, W. E. *J. Am. Oil Chem. Soc.* **1961**, 38, 199–201.

(34) Chapman, D. *J. Am. Oil Chem. Soc.* **1960**, 37, 73–77.

(35) Dyer, J. R. *Application of Absorption Spectroscopy of Organic Compounds*; PrenticeHall: Upper Saddle River, NJ, 1965; pp 36–37.

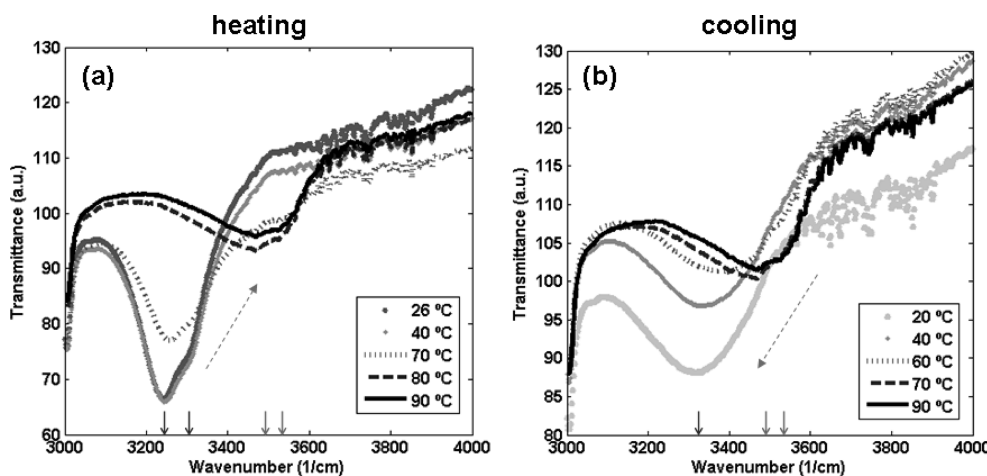


**Figure 6.** The absorption peaks in the infrared spectrum show the states of hydrogen bonding. (a) The hydrogen bonds are broken by heating. The absorption peaks therefore shift from 3250, 3350, to 3500 and 3550 (1/cm) (b) On cooling, the hydrogen bonds change their configuration below the gelation temperature (the isotropic–lamellar transition). The 3-OH hydrogen bonds are formed with the absorption shift to 3350 (1/cm). Continuously cooling down from the inverse-lamellar into the sub- $\alpha$  crystal phase, we find no change in the state of hydrogen bonding.

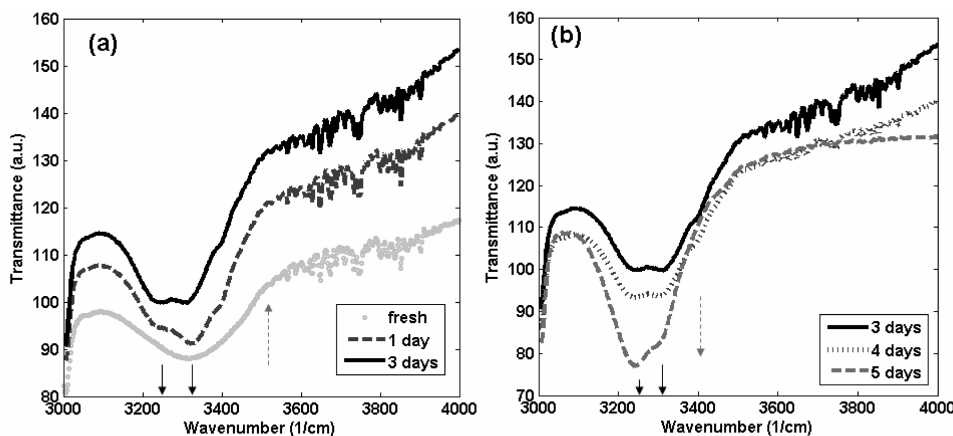


**Figure 7.** (a) During aging, the hydrogen bonding absorption peak gradually splits into two. The upper wavenumber line corresponded to 3-OH hydrogen bonds, while the lower wavenumber line is related to the lower-energy 2-OH hydrogen bonds. (b) After five days of aging, the ordered 2-OH hydrogen bonds continuously grow and finally begin to dominate.

separation of D- and L-layers. This reordering process is the key to the aging phenomena we observed on macroscopic scale.

## 5. Metastability of Inverse Lamellar Phase

The observations and the logic of our arguments about reconfiguration of hydrogen bonding being the cause of eventual establishing of the well-ordered  $\beta$ -crystal form suggest that we examine the aging of the higher-temperature inverse-lamellar phase. From the point of view of infrared absorption, there is no difference between it and the fresh sub- $\alpha$  phase. We follow the same sequence of experimental techniques.

Figure 8 shows the typical microstructure obtained by polarized optical microscopy at fixed temperature (45 °C), separated by a long period of aging. In order to record clear images, the sample thickness was less than 0.5 mm. Similar to the process in the sub- $\alpha$  crystalline phase, the samples were annealed at 100 °C and then cooled down to 45 °C, after which the texture was recorded every 3 h for two days and subsequently every 12 h for two weeks. In the inverse lamellar phase, MG initially aggregates to form dispersed lamellar bilayer plates, which made a percolating network to form a gel and trap the oil inside its structure. This texture shows bright birefringence under crossed polarizers. The size of every elongated plate domain is roughly 100  $\mu\text{m}$  in

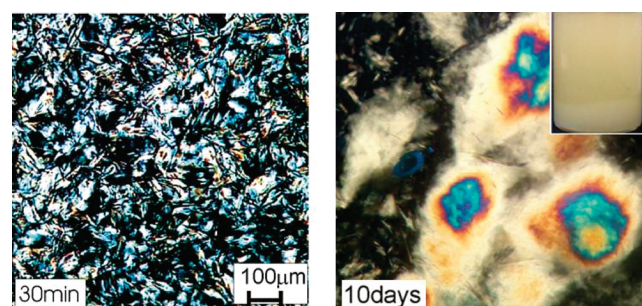


**Figure 8.** Micrographs of the inverse lamellar phase obtained by polarized microscopy. After 10 days, MG lamellar network would break and form the large structures surrounded by feather-like crystallites.

length and 25  $\mu\text{m}$  in width, the same as in the fresh sub- $\alpha$  crystalline phase. After 10 days of aging, this network is broken and large aggregates (200–600  $\mu\text{m}$ ) with a granular center surrounded by feather-like crystallites were observed.

The inverse lamellar ordering with hexagonal head-packing of MG/oil mixtures occurred between 37 and 53 °C. Aging was observed in this phase as well and was even faster than the corresponding process in the sub- $\alpha$  crystalline state. We attribute

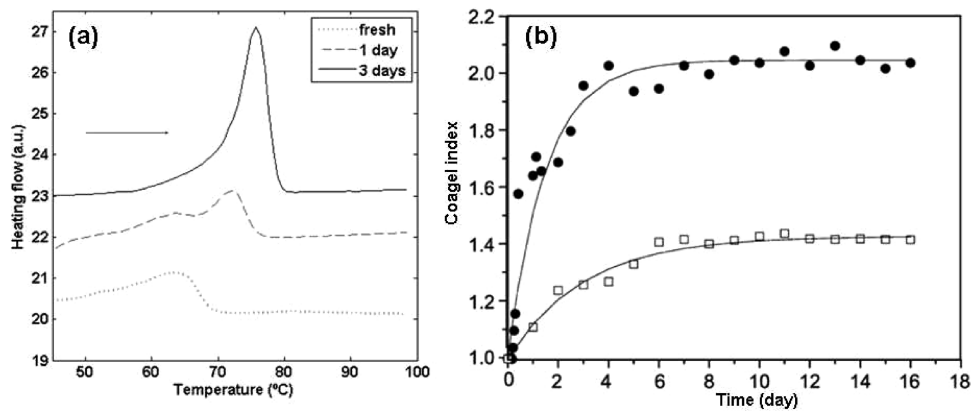


**Figure 9.** (a) During the first two days, we find two melting temperatures in the DSC heating scans: the lower one corresponds to the melting of inverse lamellar ordering, while the higher is related to the melting of the emerging  $\beta$ -crystal. After three days, the  $\beta$ -crystal ordering predominates and the melting enthalpy doubles. (b) In the inverse lamellar phase ( $45\text{ }^\circ\text{C}$ , ●), CI increased dramatically and then saturated after three days, in contrast to the smaller increase of CI in the aging sub- $\alpha$  phase ( $26\text{ }^\circ\text{C}$ , □). Solid lines represent fitting with the exponential function (see text).

the increased aging rate simply to the higher mobility of MG molecules in the lamellar phase. In order to quantify the kinetics of aging, samples stored at  $45\text{ }^\circ\text{C}$  were used in these experiments. Similar to the procedure used in the sub- $\alpha$  crystalline phase, the DSC heating scans were taken from  $40$  to  $100\text{ }^\circ\text{C}$  of the samples with different storage time (see Figure 9a). The increase of latent heat was calculated to obtain the evolution of the coagel index (see Figure 9b). This procedure is prone to high errors at the early stages of aging, because we are starting the scan from a temperature that often is in the middle of the second transition, and it is hard to calculate the enthalpy change with precision. Once the two transitions merge after a long period of aging, the calculation of coagel index becomes much more accurate.

The results of infrared spectroscopy reveal that, in the early stage of aging, hydrogen bonds drive the restructuring of lamellar bilayers. Calorimetry confirms these conclusions. During aging, the sample was partially crystallized, and so two melting peaks occur. The lower-temperature transition corresponds to the melting of remaining lamellar ordering, while the emerging transition at the upper temperature indicates the melting of the  $\beta$ -crystals. On aging, the intensity of the upper peak increased, and the lower peak gradually disappeared. After three days, the upper melting transition became dominant. The material was fully aged to the  $\beta$ -crystalline state; hence, the big increase in the coagel index occurred.

To compare the aging process in crystalline and lamellar phases, the evolutions of CI in both phases are plotted in Figure 9b. In both cases, this increase could be represented by the exponential relaxation function:  $\text{CI} = 1 + X(1 - \exp(-t/\tau))$ , where  $X$  is a fitting constant and  $\tau$  the relaxation time. In the sub- $\alpha$  crystalline phase, the best fit was achieved with the amplitude  $X = 0.43$  and the relaxation time  $\tau = 3$  days. The evolution of the CI in the inverse lamellar phase fit with  $X = 1.05$  and  $\tau = 1.5$  days. We conclude that the aging process in the inverse lamellar phase is much faster than in the sub- $\alpha$  crystalline state.

Figure 9b also shows different shifts of CI during aging in the sub- $\alpha$  crystalline and inverse lamellar phases. In the sub- $\alpha$  crystalline phase, D- and L-isomers change their arrangement within crystalline bilayers and the CI increased from  $1.0$  to  $1.4$ . In contrast, the aging process in the inverse lamellar phase had to experience two steps of ordering. The first step is the crystallization of aliphatic chains in their all-trans conformation, while the second step involves the rearranging of D- and L-isomers similar to the aging in the crystalline phase. By summing the

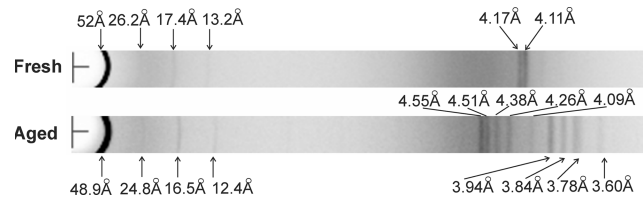


**Figure 10.** Restructuring during the aging of the inverse lamellar phase is monitored by X-ray scattering. In the fresh lamellar phase, the wide-angle peaks show the packing of glycerol groups in a 2D hexagonal manner.<sup>5</sup> During aging, the wide-angle structure breaks into two series of peaks, which are identical to the triclinically packed  $\beta$ -crystal.

entropy change from step one and step two, CI increased to  $2.0$ . As expected, during aging of the inverse lamellar phase the increasing of CI is larger than in the sub- $\alpha$  crystalline phase.

In order to describe the aging of microstructure in the inverse lamellar phase, X-ray diffraction results are shown in Figure 10. As always, there was a series of concentric rings in the small-angle region to show the existence of lamellar ordering in both fresh and aged materials. Here, one observes the decrease of the bilayer periodicity on aging, due to their gradual crystallization. The difference between the phases is more clearly revealed by the wide-angle diffraction. As expected, the fresh inverse lamellar phase only gives the twin short spacing X-ray peaks at  $4.17$  and  $4.11\text{ \AA}$ , characterizing the 2D hexagonal head packing in the middle of each bilayer.<sup>5</sup> After three days, the wide-angle scattering pattern developed two series of peaks, which was identical to the  $\beta$ -crystalline state (3D triclinical arrangement) described in Figure 5 before. This result confirms that the inverse lamellar phase was in fact metastable and eventually transforms to the  $\beta$ -crystalline state. Although the aging process of the lamellar and sub- $\alpha$  crystalline phases are different, both of them aged to the same stable  $\beta$ -crystalline phase eventually.

## 6. Conclusion

The phase behavior of MG/oil mixtures is summarized in Figure 11. Importantly, all our studies were carried out in the absence of water, which would be expected to have a pronounced effect on hydrogen bonding even in small quantities. As reported earlier,<sup>5</sup> there are four generic phases in this system: isotropic, inverse lamellar, sub- $\alpha$  crystalline, and  $\beta$ -crystalline phases. The study of aging, which takes place in the inverse lamellar and in the sub- $\alpha$  crystalline phases, constituted the bulk of this paper.

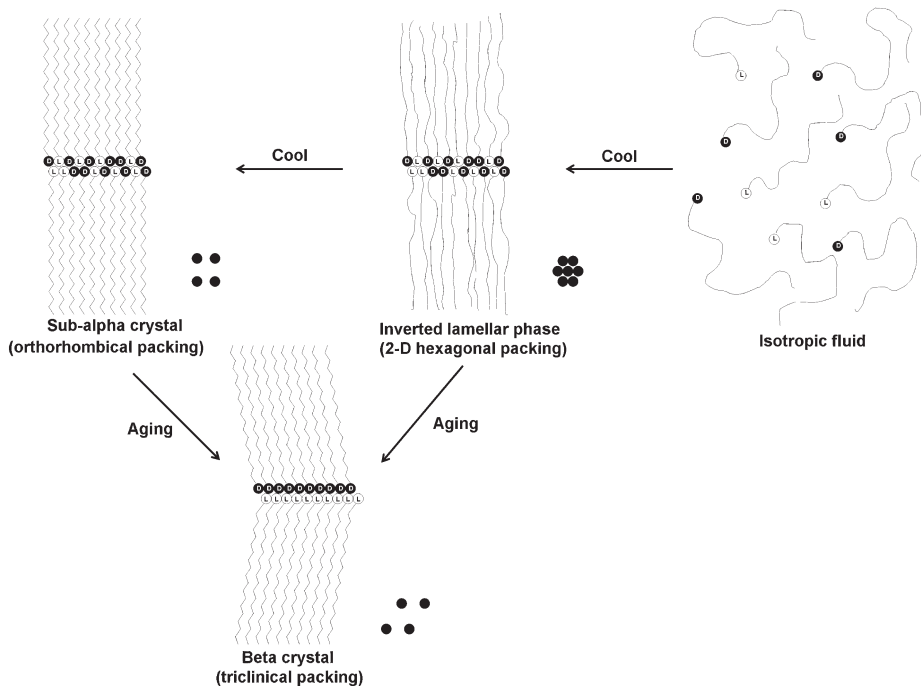


**Figure 11.** Four phases of MG/oil mixtures: isotropic, inverse lamellar (2D hexagonal head packing), sub- $\alpha$  crystalline (3D orthorhombic packing), and  $\beta$ -crystalline (3D triclinic unit cell). On aging, 2-OH hydrogen bonds between the polar glycerol head groups are formed and lead to the regular stacking of D- and L-isomers into the equilibrium structure of  $\beta$ -crystal. Both inverse lamellar and the sub- $\alpha$  crystalline phases are thus metastable and transform into the  $\beta$ -crystalline state on aging.

Optical microscopy, calorimetry, X-ray diffraction, and infrared spectroscopy results were presented to provide a comprehensive set of both macroscopic and microstructural characteristics of aging.

In order to quantify the aging process, a dimensionless parameter called the coagel index (CI) was defined<sup>1,3</sup> to represent the relative increase in the order and thermodynamic stability of phases. Here, the CI was recorded by DSC to trace the kinetics of aging. In the sub- $\alpha$  crystalline phase (at 26 °C), the aging process needed five to seven days to achieve a saturated state of highly ordered  $\beta$  crystal in which 3-OH hydrogen bonds were fully established. In order to establish the relationship between aging and the hydrogen bonding, the time evolution of infrared spectra had been examined. The coexistence of 3- and 2-OH hydrogen bonding was observed in the initial stages of aging, while the 2-OH hydrogen bonding was dominant and led to the separation of D- and L-isomers as a result of aging. We need to emphasize that the conclusion about chiral isomer separation is not a specific result of our investigation: what we have done unambiguously is to identify the  $\beta$ -crystalline state as the final destination of aging process; there is extensive literature (using a variety of chirality-sensitive techniques) that confirms that this  $\beta$ -crystal is made of separated enantiomers (see ref 1 and references therein).

Structural studies confirm the 3D triclinic packing in the  $\beta$ -crystalline phase. Two groups of X-ray reflections reflect the

crystallization of carbon chains and the regular packing glycerol heads, respectively. The separation and reordering of D- and L-isomers weakens the emulsifying ability of MG aggregates and causes the metastability of the gel network. The results lead us to the conclusion that both lamellar (2D hexagonal head packing with a dense fully extended brush of disordered aliphatic chains) and sub- $\alpha$  crystalline (3D orthorhombic packing) phases are in fact metastable and eventually transform into the  $\beta$ -crystalline state (3D triclinic packing), which has a high melting point.

Saturated monoglyceride in oil make a very rare system that forms an elastic gel immediately after ordering from the isotropic phase. However, with the time of aging the emulsifying ability is lost, leading to separation of oil and densely aggregated crystalline lipid. Hopefully, the results of this work will help in better understanding of the long-term behavior of MG in hydrophobic environment and improve their use in relevant technologies.

**Acknowledgment.** We gratefully acknowledge S. M. Clarke, I. van Damme, B. Sun, and A. R. Tajbakhsh for useful discussions and guidance. The help of D. Y. Chirgadze in obtaining the SAXS X-ray data is gratefully appreciated. This work has been supported by Taiwan Government Scholarship to study abroad by the Ministry of Education, Cambridge Overseas Trust, and Mars U.K.